Continuation of necessary corrections of the mathematical foundation of fracture mechanics

Continuation of the published main article under this name

T.A.C.M. van der Put[*]

TU-Delft, Civil Engineering and Geosciences, Wood Science c/o Section Biobased Structures and Materials
c/o Wielengahof 16   NL2625 LJ Delft, The Netherlands

ABSTRACT

Discussed are necessary theory extensions and clarifications of applied errors in fracture mechanics, mentioned, in the former published main article under the same name. In the main article is shown, that the general applied fracture mechanics textbook crack tip boundary value problem solution is not all right, not only regarding boundary conditions and transformation, but also by applying together, the exact Stevenson's potentials solution for tension mode I loading alone and for shear, mode II loading alone, which exclude each other and can not act at the same time and therefore don't satisfy compatibility and equilibrium conditions nor the mixed mode failure criterion, which is the necessary solution of a boundary value problem analysis for all possible, at the same time, acting loading. Further, the given stress equations only apply for lower order distances to the crack tip singularity (which are several orders lower than the crack length) and lead to meaningless higher order stress equations. To correct this, an alternative limit analysis derivation of the "mixed I-II-mode" fracture criterion is proposed, which is verified to show a high precision by empirical research. The necessary limit analysis approach for failure, as exact calculation method, provides the necessary linear elastic analysis up to failure. Linear elastic stress and displacement terms are shown to represent the none vanishing first order row expansion terms of virtual work and displacement behavior, of any non-linear stress division. The discussion is further extended regarding the small values approach; the transformations; the derivation of the hydrostatic stress, failure state at the right boundary value conditions; the determining parameters of the fracture equations, which e.g. determine the crack tip opening displacements and e.g. show the need to account for the crack length as well as the crack width. For comparison and to account for the special form of the elliptic crack surface, an alternative solution is followed by keeping the fracture equations in elliptical coordinates and writing only the end result in Textbook vocal coordinates. Further, an extension is given of the *high stress critical stress intensity by including a process zone correction of the crack length. .*

*corresponding author, Tel: +31 152851980, E-mail: vanderp@xs4all.nl

INTRODUCTION

Additional comment is given on the discussion started in [1], showing the untenable mathematical approach of textbook stress and strength calculations. Except correction of mathematical errors, and schematization there is no need to apply non-linear fracture mechanics at high stresses. Linear elastic strain determines the applied stress level and linear elastic behavior, up to the ultimate state, as applied in limit analysis, cannot be missed in linear and non-linear fracture mechanics. As shown in the main text [1], illustrated by the there given figures 2 and 3, applies for loading a test-specimen to a chosen ultimate state level, after passing through a damage and confined plastic stage, that the next unloading and reloading stages are linear elastic. The stress division then is linear elastic plus an internal equilibrium system, which does not affect collapse, according to limit analysis theorems, when the original coordinate dimensions are retained in the calculation (as always is applied). The possible elementary linear elastic approach up to failure, is the consequence of application of the virtual work approach of limit analysis. To avoid configurational changes, virtual work and virtual displacements have to be applied in analyses or only first expanded of the load, displacements and stress division apply, because second and higher order quantities are zero in the virtual limit. Or, what is the same, the linear elastic approach has to be followed and for that reason design also should be based on the first expanded of a Fourier expansion of the load, as e.g. in [2], and as prescribed by the Eurocode. A lower bound solution then is based on equilibrium equations and stress boundary conditions, which nowhere violate the yield condition. When this solution shows no discontinuity of displacements, the solution also is the exact solution. When there is an empirical confirmation, no upper bound estimation is needed and is not applied in practice. See [1] eq.(5.1) to (5.10). The textbook equations and derivations are based on small values of variables and dimensions as applies for flat cracks near the crack tip. However, this approximation should be done at the end of the derivation and not at the start, as is done, because that clearly lead to errors which will be corrected in the following.

DISCUSSION OF GENERAL APPLIED STRESS EQUATIONS

determining hydrostatic stress state occurs at that point and shows to be always determining As shown in [1], the general applied fracture mechanics stress equations, as presented in [3] appendix 2, are based on Stevenson's Airy stress function solution [4]-§ 8.10 for pure mode I, thus tension perpendicular to the crack direction alone, applied together with the solution of pure mode II alone, thus pure shear loading along the crack alone, although these solutions are not compatible and exclude each other and can not apply at the same time. Thus not the mixed mode I -II solution is regarded, of which these two mono mode solutions are special cases of mono mode loading. Also the real boundary value solution along the whole crack in an infinite plate, regarding first order stresses along the crack border, as well as at infinitum, what leads to the exact solution [1]-eq.(4.13), is not followed. In stead, only the partial mono mode solutions, leading to equal undeterminable high full hydrostatic stresses near the crack tip, are regarded, based on a transformation of the elliptical coordinates of the potentials into a polar coordinate system, centered at one of the two elliptic focusses of the elliptical crack, which show to be not right for $\theta > 0$ for the applied pure small values of variables and distances approach.

Stresses near the crack tip

As mentioned in [1], the, by Textbooks applied, crack boundary value solution is restricted to the analysis of stresses at one, of the two, crack tips, of an elliptic crack in an elliptic confocal coordinate system, as given in [4]- §8.10, and also discussed at [1]- eq.(6.1) to (6.25). Thus not is, as normal, the whole crack boundary regarded. The applied loading cases consist of one principal stress at an angle β to the crack direction, one principal stress at $\beta = \pi/2$, as mode I loading and the pure shear loading case. The general loading case of one load, inclined at β to the crack direction Ox, with a second load at an angle $\beta + \pi/2$, making any load combination possible, is not regarded. By that, the necessary general mixed mode I -II solution, which includes pure mode I and pure II loading cases, is not obtained. As necessary correction this mixed mode derivation is discussed in [1]– eq.(4.1) to (4.13) and eq.(5.1) to (5.10).

The stress estimation is already, from the start of the derivation, based on small values approximations of variables, distances and flat crack tip dimensions, being several orders lower than the crack length and thus only reliable on that scale. Therefore it is not possible to account for crack symmetry conditions of place and stress. This is shown in [1], starting at [1]-eq.(6.1). These equations, applied in all Textbooks show an increasing distortion with

θ and the lower δ in Fig. 1 is wrongly taken to be θ in stead of $\theta/2$ in [3]. Thus elliptic coordinate equations are associated with a non-elliptic surface.

In the analysis: $\theta \approx 0$ is determining. The only reliable critical value thus is obtained at the crack tip, thus at $\theta = 0$ and for near zero r of the flat sharp cracks. Thus general applied equations, as e.g. [1]-(6.19) to (6.21) and (6.26) to (6.28) only apply for $\theta \approx 0$. The application of these equations for higher values of θ, explains the obtained increasing mathematical errors of the principal stress values with the increase of θ.
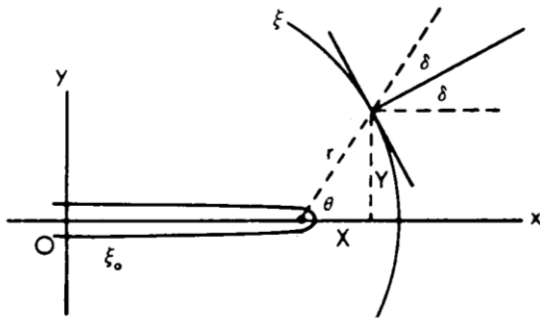

Figure 1.- Confocal polar coordinates for transformation of the elliptical crack coordinates to polar crack tip coordinates at an elliptic focus.

Equations [1]-(6.15) to (6.17) are for one stress field p at an angle β to the crack. As necessary correction, the general loading case is given by a two-dimensional stress σ_1, σ_2 inclined at $(\pi/2 + \beta)$ and β to the crack direction. This may represent any general loading system. This therefore is applied, with the right boundary conditions, in the exact derivation for mixed mode failure, at [1]-eq.(4.7). The right boundary conditions are not regarded in all textbook approximations. The loading cases, by the focal polar coordinates transformation of the solution in elliptic coordinates, are the pure mode I loading perpendicular to the crack direction ($\beta = \pi/2$) and the mode II, pure shear, loading along the crack. As discussed in [1] at eq.(6.26), this mode II solution is not right, and wrongly the determining hydrostatic stress state in elliptical coordinates is disappeared by this small values transformation to focal polar coordinates. The discussion of the pure mode I loading case is given at [1]-eq.(6.18). The highest, assumed critical, tensile stress occurs at $\theta = 60^\circ$. But, mode I crack extension is collinear, thus occurs at $\theta = 0$. This is the case, because the strength.

Below [1]- eq.(6.11) is mentioned that the term: $p \cdot \cos(2\beta)$ always is regarded to be negligible with respect to: $p \cdot (c/2r)^{1/2} \cdot (2) = p \cdot (2c/r)^{1/2}$. Thus $p \cdot (2c/r)^{1/2}$ should be one order

4

higher than p, or: $2c/r$ should be 2 orders higher than order one. Thus maximum radius r_o should be less than 1/100 times the crack length $2c$. The derived equations thus consist of higher order stresses, indicating that not stresses but stress intensities have to be applied. In the ultimate stress equations is $r = r_o$, the distance of the nearest elliptical focus to the crack tip boundary, where crack extension will proceed. For flat sharp cracks, which are regarded, is r_o very small. Further, only lower order elliptic coordinate values ξ and η are accounted, which apply near the crack tip. This follows e.g. by the derivation in [1]- eq.(6.11). Regarded is e.g. $\sinh(2\xi) \approx 2\xi$ and $\sin(2\eta) \approx 2\eta$ which next are regarded to be equal to: $\xi = (r/c)^{1/2}\cos(\theta/2)$ and $\eta = (r/c)^{1/2}\sin(\theta/2)$. This means that r/c is 2 orders lower than the lower order values ξ and η, thus is extremely small. For the determining fracture at the crack tip, applies $\eta = 0$ and $\theta = 0$ which are coordinate values of the crack tip. In the derivation also $\xi_o = 0$ is introduced so that then $p \cdot \cos(2\beta)$ in eq.(6.11) indeed is several orders lower and has to be omitted. Constant $\xi = \xi_o$, is an elliptic hole with semi-axes: $a = c \cdot \cosh(\xi_o)$, $b = c \cdot \sinh(\xi_o)$, which may represent the first expanded of any crack form. Because ξ is small, ξ_o is smaller and is taken to be zero where possible in the derivation. This means that the crack is a closed slit, thus the crack width $b = 0$. Then also $\sqrt{(r_o)}$ in [1]- eq.(6.5): $\xi_o = (2r_o/c)^{1/2}$ has to be taken to be zero. This means that the always presented stress equations in appendix 2 of [3] and equations (8.246) to (8.275) of [4], all with r_o in the denominator, show not measurable undetermined high hydrostatic stresses, thus are in the given form meaningless and should be given as stress intensities. Then is, for instance Eq.(8.253) of [4], for mode I, thus for $\theta = 0$: $\tau_{\theta\theta} = \sigma_\perp(c/2r)^{1/2}\cos^3(\theta/2) = \sigma_\perp(c/2r)^{1/2}$. Thus:

$$\sigma_\perp \cdot (\pi c)^{1/2} = \tau_{\theta\theta} \cdot (2\pi r_o)^{1/2} \quad \text{or: } K_I = K_{Ic} = K_{IIc} ? \tag{1}$$

All mentioned equations in [4] and [3] predict that the critical stress intensities for mode I and mode II are equal. The cause of this error is the lack of application of the right boundary conditions at pure hydrostatic tension failure. The predicted equal stress intensities may apply in the field, e.g. in the fracture process zone, but not at, or adjacent, to a critical crack. For failure at the crack boundary $x = x_o$, the boundary conditions (of Griffith) are: $\sigma_t = \sigma_\eta$ for the tangential stress in the crack surface and $\sigma_\xi = 0$ for the stress perpendicular to the crack direction. Because the crack is empty, the normal stress to the crack boundary is zero what also applies for the shear stress in the crack surface. This is mentioned below [1]- eq.(4.5) and is accounted for the derivation of the mixed mode fracture criterion, [1]- eq.(4.13) which therefore is given. It follows that $K_{Ic} = \sigma_t \cdot (\pi r_o /2)^{1/2}$ and $K_{IIc} = \sigma_t \cdot (2\pi r_o)^{1/2}$. Thus $K_{Ic} = 0.5 \cdot K_{IIc}$ for isotropic material, as empirically is verified. For orthotropic wood

K_{IIc} / K_{Ic} is roughly about 8 times higher, depending on the species. See [1]- eq.(5.1) to eq.(5.10) and also [2] for the derivation.

Main stress deviations by the applied focal coordinate system

The main deviation with the exact approach is that the general loading case of combined tension perpendicular to the crack with shear along the crack, is not regarded in Textbooks. By that, the necessary determining critical stress state of combined mixed I - II mode failure is not obtained. Further, only small scale variables and small distances, several orders lower than the crack length $2a$, are regarded. This leads to errors, when these equations are applied on full scale as is done. For pure shear loading along a crack, there are two principal stresses at infinity, one stress p inclined at $\beta = \pi/4$ to the Ox crack axis, and the other negative stress $-p$ inclined at $\beta = 3\pi/4$. It appears that, with the increase of θ, an increasing hydrostatic tensile stress state is superposed, up to p at $\theta = \pi$, what results to one zero principal stress and one principal stress of $2p$. The same occurs on pure mode I loading, where at $\theta = 0$, there is a hydrostatic stress state of stress p, and where for $\theta = \pi$, an opposite hydrostatic stress state of p is superposed, leading to all zero stresses: $\tau_{r\theta} = \sigma_{\eta} = \sigma_{\theta} = 0$. Because the very small scale, equations only apply for $\theta \approx 0$, there thus is no need to apply a focal polar coordinate system. The determining tangential stress σ_{η} of the general, thus mixed mode, loading system is directly known by differentiation of the potential for the tangential stress as is applied for the derivation of the mixed I-II -mode equation. This delivers the right boundary conditions, which are wrongly ignored by the Textbooks.

Hydrostatic stress state for mixed mode fracture at the right boundary conditions

The derivation of the hydrostatic stress state in general, for local critical field stresses, is given at: [1]- eq.(4.14) to eq.(4.27). Eq.(4.14) and eq.(6.18) of [1], give the mode I, at the crack tip ($\theta = 0$), determining maximal hydrostatic stress ($\sigma_{\theta} = \sigma_r$), at the right boundary conditions. For pure mode II (shear), this does not apply and the hydrostatic stress state is Disappeared by the transformation. This certainly is due to the applications of small variables at the start of the derivation in stead of at the end, because the transformation in textbooks, from elliptic to focal polar coordinates, is exact, by applying the transformation equations. The derivation of the mode II hydrostatic stress in elliptic coordinates is given in [1]- eq.(4.21) to eq.(4.27). As shown is for the condition $\sigma_{\xi} = \sigma_{\eta}$: $\cosh(2\,\xi) = \alpha/(\alpha - 1)$ and for the condition $\tau_{\xi\eta} = 0$: $\cos(2\,\eta) = \alpha/(\alpha + 1)$ or because $\alpha \gg 1$ is for de first expanded:

$\cosh(2\xi) = \alpha/(\alpha - 1) = 1/(1 - 1/\alpha) \approx 1 + 1/\alpha = 4\xi^2/2 + 1 \rightarrow 2\xi^2 = 1/\alpha$ and

$\cos(2\eta) = \alpha/(\alpha + 1) = 1/(1 + 1/\alpha) \approx 1 - 1/\alpha = 1 - 4\eta^2/2 \rightarrow 2\eta^2 = 1/\alpha$. Thus:

$\eta = \xi = \sqrt{(1/2\,\alpha)} = \sqrt{(2r/c)}$.

This agrees with eq.(6.5) and (6.6) of [1], because small variable $\theta \approx 0$. At the crack tip is:

$\theta = \eta = 0$.

For the determining fracture at the crack boundary, in mixed mode I -II, the right boundary conditions at the border of an empty crack have to be applied. This equation, which follows from the tangential stress equation at the crack boundary, thus accounting for the right boundary conditions, is eq.(4.13) of [1]:

$$\frac{\sigma_y \sqrt{\pi c}}{\sigma_t \sqrt{\pi r_0/2}} + \frac{\left(\tau_{xy}\sqrt{\pi c}\right)^2}{\left(\sigma_t\sqrt{2\pi r_0}\right)^2} = \frac{K_I}{K_{Ic}} + \frac{K_{II}^2}{\left(K_{IIc}\right)^2} = 1$$

and it follows that: $K_{IIc} = 2 K_{Ic}$. In this mixed mode fracture equation is r_o the distance of the focus to the nearest crack tip, where crack extension will proceed. Also is $r_o = \rho/2$, where $\rho = b^2/a$ is the radius of the crack tip, thus $1/\rho$ is the crack tip curvature.

The more general equation [1]- (4.7) of the tangential stress σ_t at the crack boundary $\xi = \xi_0$, loaded by two stresses σ_1 and σ_2 inclined at $(\pi/2 + \beta)$ and β to Ox also is:

$$\sigma_t = \frac{2\sigma_y \sinh(2\xi_0) + 2\tau_{xy}[(1 + \sinh(2\xi_0))\cot(2\beta) - \exp(2\xi_0)\cos(2(\beta - \eta))\cosec(2\beta)]}{\cosh(2\xi_0) - \cos(2\eta)} \quad (2.1)$$

This can be given in the principal stresses according to:

$$\sigma_x = \sigma_1 \sin^2(\beta) + \sigma_2 \cos^2(\beta) \quad \sigma_y = \sigma_1 \cos^2(\beta) + \sigma_2 \sin^2(\beta) \quad \tau_{xy} = -0.5(\sigma_1 - \sigma_2)\sin(2\beta)$$

$$\sigma_t = \frac{(\sigma_1 + \sigma_2)\sinh(2\xi_0) + (\sigma_1 - \sigma_2)[\exp(2\xi_0)\cos(2(\beta - \eta)) - \cos(2\beta)]}{\cosh(2\xi_0) - \cos(2\eta)}$$

σ_t is maximal when $\eta = 0$, thus at the crack tip, and because ξ_0 is very small and taken to be zero (as slit with crack width $b = 0$), is: $\exp(2\xi_0) \approx 1$, what leads for hydrostatic stresses:

$\sigma = (\sigma_1 + \sigma_2)/2$ or full hydrostatic: $\sigma_1 = \sigma_2 = \sigma$, to:

$$\sigma_t \approx \frac{(\sigma_1 + \sigma_2)\cdot(2\xi_0)}{2\xi_o^2 + 2\eta^2} = \frac{2\sigma}{\xi_0}$$

Thus: $\sigma_t = 2\sigma/\xi_o = 2\sigma\cdot\sqrt{(c/2r)}$, and: $K_I = \sigma\sqrt{(\pi c)} = K_{1c} = 0.5\cdot\sigma_t\sqrt{(2\pi r_o)}$. Thus $K_{1c} = 0.5\ K_{IIc}$.

For high, pure hydrostatic part of the principal tensile stresses $\sigma_1 = \sigma_2 = \sigma_3 = \sigma$ and $\sigma_3 = \nu\sigma_1 + \nu\sigma_2 = \sigma$. Thus $\nu = 0.5$ for no volume change and $\tau_{xy} = 0$. This is possible, according to the, for the isotropic wood matrix applying, critical distortional energy principle. High hydrostatic stress is also measured in materials. Measured is e.g. 60

atmospheres for tension of water in a glass tube. How high would this be in a perfect tube at a perfect load application. The semi-log-plot, according to molecular deformation kinetics, [5], of crack speed data, indicated a high apparent activation energy, which was high enough for molecular -C-O- bond breaking of wood polymers. Thus the occurrence, of the hydrostatic state in one point, gives the start of a hydrostatic stress field extension in the same way as Irwin's plastic stress field extension starts elastic locally.

It is not noticed in Textbooks, as e.g. in [3] and in [4]- § 8.10, that, by not applying the right boundary conditions, the found critical stress intensities, for mode I and II, are wrongly predicted to be equal. This has to be mentioned because it is against empirical data.

Parameters of strength and fracture equations

In eq.(2.1) and in eq.(2.5) is, for sharp flat cracks:

$$\xi_0 \approx b/c \approx b/a \tag{2.2}$$

where b and a are the major semi axes of the elliptic crack in the elliptic coordinate system and c is the semi focus distance, which for flat cracks is: $c \approx a$, the open crack length. In strength theory the crack width b is not separately accounted and $\sigma_t \cdot b/a$ is measured as the common, order one, apparent tensile strength. This is based on, always the same initial small cracks, thus the same very high hydrostatic stress σ_t and very small b/a of the initial small clear-wood notches. For the analysis of crack propagation behavior, is necessary, to account for the small crack width b, and for the apparent crack length, including the fracture process zone length and for the stress intensity fracture criterion. Further, the extend of the fracture process zone, as hydrostatic tension field, has to be known.

The radius ρ of the curvature of the elliptic crack tip at $x = a$ is: $\rho = b^2/a$. Thus is:

$$\sigma_t \cdot b/a = \sigma_t \cdot \sqrt{\rho/a} \tag{2.3}$$

with ρ as radius or: $1/\rho$ the curvature of the crack tip.

Transformation from elliptic- to confocal polar coordinates, by eq.(6.5) of [1], gives:

$$\xi_0 = \sqrt{2r_0/c} \cdot \cos(\varphi) \approx \sqrt{2r_0/c} = b/c = \sqrt{\rho/c} \approx \sqrt{\rho/a} \tag{2.4}$$

where r_0 is the distance of the nearest focus to the highest stressed point at the crack boundary, which is situated near the crack tip ($\varphi \approx 0$) and substitution in eq.(2.1) gives, for variable c, and constant $\sigma_t (r_o)^{1/2}$:

$$\frac{\sigma_y \sqrt{\pi c}}{\sigma_t \sqrt{\pi r_0 / 2}} + \frac{\left(\tau_{xy} \sqrt{\pi c}\right)^2}{\left(\sigma_t \sqrt{2\pi r_0}\right)^2} = \frac{K_I}{K_{Ic}} + \frac{K_{II}^2}{\left(K_{IIc}\right)^2} = 1 \tag{2.5}$$

what is the mixed I-II mode fracture criterion, also for orthotropic wood according to eq.(5.8) of [1]. In eq.(2.5), the product $\sigma_t \cdot (r_o)^{1/2}$, determines the critical mode I and II stress intensities. The distance r_o from the focus of the elliptical crack to the adjacent critical crack tip boundary, where crack extension proceeds, is very small for flat cracks (when $a \gg b$). Thus the high apparent cohesion strength σ_t is reached, due to the indefinite high strength of the 3-dimensional pure hydrostatic stress state at the crack tip. The derivation in elliptic coordinates is given in [1] eq.(4.19) to eq.(4.27). In cartesian coordinates it appears that for any load combination, failure occurs at crack tip equal principal stresses $\sigma_1 = \sigma_2 = \sigma_3$. As shown also in [1], the general accepted textbook (e.g. Anderson 1995) mono mode stress equations, which are in format:

$$\sigma_x = \frac{K_1}{\sqrt{2\pi r}}\cos\left(\frac{\theta}{2}\right)\left(1 - \sin\left(\frac{\theta}{2}\right)\sin\left(\frac{3\theta}{2}\right)\right) \quad \text{etc} . \tag{2.6}$$

are copied equations of the stress at the crack boundary, based on Stevenson's Airy stress function solution, and apply only for the maximal value $r = r_0$, the location of this boundary, the same r_0 as given by eq.(2.5), which is at least 2 orders smaller than the semi crack length a, but still much smaller for accountable sharp, flat cracks. Eq.(2.6) thus wrongly is applied with variable r, e.g. to wrongly determine the remote r- values of the contours of the plastic zone around the crack tip.

Besides the crack length a, also the crack width b is determining for the strength. This also follows e.g. from the general applied, linear elastic estimation, of the plastic mode I crack tip opening displacement (CTOD) δ_o, (thus based in principle on a linear elastic limit analysis approach as also applies for the correlated linear elastic, and by virtual work, estimated and estimating J-integral). For plane strain this δ_o is, according to the textbooks:

$$\delta_0 = 2K_1^2 / \pi\sigma_y E \tag{2.7}$$

which is based on the effective crack length: $a + r_y$ including the length r_y behind the effective crack tip e.g. according to Irwin's plastic zone correction.

Eq.(2.7) can be written, after inserting K_1 of eq.(2.5):

$$\delta_0 = 2K_1^2 / \left(\pi\sigma_y E\right) = 2\sigma_y^2(\pi r_0 / 2) / \left(\pi\sigma_y E\right) = r_0\sigma_y / E = r_0\varepsilon_y = \rho\varepsilon_y / 2 \tag{2.8}$$

Thus the CTOD δ_o at first yield ε_y is proportional to r_o and thus to $\rho/2$ according to eq.(2.10), and thus to b^2 according to eq.(2.9). In this CTOD model, r_o is the radius of the circular assumed crack tip. However r_o is extremely small for sharp cracks showing the CTOD to be not measurable and also to be a superfluous parameter. It is accounted in the form of r_o or ρ as follows:

9

According to eq.(2.4) is: $\xi_o = \sqrt{(2r_o/c)} \approx \sqrt{(2r_o/a)}$ and is, for an ellipse, equal to: $\xi_o = b/a$ or:

$$r_0 = b^2 / (2a) \tag{2.9}$$

The radius ρ of the curvature of the elliptic crack tip at x = a is: $\rho = b^2/a$. Thus is:

$$\rho = 2r_0 \tag{2.10}$$

and $2r_o$ in eq.(2.5) can be replaced by ρ, giving the influence of the sharpness of the crack tip and thus also of crack blunting.

Extension of the boundary value crack tip curvature solution of Inglis

According to eq.(2.1) is the highest stress for mode I fracture at the crack tip:

$$\sigma_y = \sigma_t \frac{\xi_0}{2} = \sigma_t \sqrt{\frac{r_0}{2c}} = \sigma_t \sqrt{\frac{\rho}{4a}} \tag{2.11}$$

This is identical to the result of the single mode I boundary value derivation of Inglis [6] in 1913, (applied by Griffith for his ultimate stress, strength criterion and to evaluate the strain energy of his additional energy approach). According to the linear elastic crack boundary value analysis of Inglis, shown in all textbooks, follows for mode I failure:

$$\sigma_t = \sigma_y \left(1 + 2\sqrt{\frac{a}{\rho}}\right) \approx 2\sigma_y \sqrt{\frac{a}{\rho}} \tag{2.12}$$

for sharp flat cracks. Thus, reversed is:

$$\sigma_y = \sigma_t \sqrt{\frac{\rho}{4a}} \tag{2.13}$$

what also follows from eq.(2.1) or eq.(2.5) which are based on Stevenson's Airy stress function solution. Thus the derivation of Inglis, for single modes failure, is shown to be extended for mixed I-II mode failure by eq.(2.5) for any load combination. It also is shown that Stevenson's Airy stress function solution, and the displacement functions solution of Inglis, lead to the same stress equations, at the critical crack boundary. Both solutions are complete and exact by calculating displacements, which should show no displacements discontinuities.

Equation (2.5), also is equal to the empirical Wu-equation, which is the only equation that is not rejected by the lack of fit test (See [1], Table I). Wu [7] noticed a crack jumping over fibers, what is identical to fracture propagation at an alternate, but small, changing value of (+ and -) φ, which thus is neglected as best value. As shown, fracture always ends at φ, of eq.(2.4), to be close to zero by failure of the developed hydrostatic bonds in the end state. For clear wood and short rectangular notches, however, the mathematical, by maximal

stress predicted, oblique crack extension is possible [8], when shear loading is involved, as also is measured, what is discussed in [2]. Eq.(2.5), as exact equation, also follows from the critical distortional energy principle [2], thus also applies for initial flow before building up a hydrostatic stress field (as fracture process zone) at the crack tip. The consequence that this principle applies to wood means that also an indeterminate high hydrostatic strength applies for the isotropic wood matrix stresses.

Extended critical stress intensity criterion

According to the exact eq.(2.5) applies for linear elastic initial mode I failure:

$$\sigma_y \sqrt{\pi c} = \sigma_t \sqrt{\pi r_0 / 2} = C \tag{3.1}$$

which shows that a critical stress intensity criterion applies for fracture and not a critical energy release rate. This is e.g. empirical confirmed by the data of [9], given in Fig.1, which are fit to eq.(3.2). The fact, that there is one fracture strength data-line for these geometrically similar specimens, shows that there is no volume effect. The reason of this is that the fracture process zone d_0, as determining high stress zone, is of about the same size, due to the same crack width or same crack tip curvature, thus proportional to r_o or b or ρ, for all specimens.

In Fig.1 is d/d_o, the ratio of specimen size d, to the constant fracture process zone size d_o. But, because the line is the result of the volume effect tests, the initial crack length is
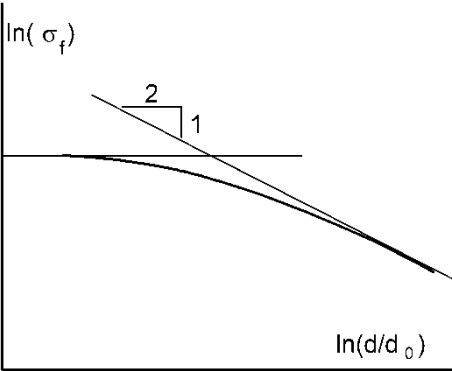
Fig. 1. Limit LEFM behavior, depending on the crack-length d = a to process zone d_o ratio showing no need to regard nonlinear fracture mechanics as is assumed for the curved part. Data of Bazant [9].

proportional to the test-specimen length. Thus, d/d_0, also can be regarded to be the ratio: initial open crack length, to the process zone size, a/d_0.

The curved strength data line of Fig.1, follows the equation:

$$\ln \sigma = \ln \sigma_0 - 0.5 \ln (1 + d/d_0) \tag{3.2}$$

This thus can be changed to:

$$\ln \sigma = \ln \sigma_0 - 0.5 \ln (1 + a/d_0) \tag{3.3}$$

or as critical stress intensity:

$$\sigma \sqrt{\pi (d_0 + a)} = \sigma_c \sqrt{\pi d_0} = K_c \tag{3.4}$$

in accordance with eq.(2.5) and eq.(3.1). The crack however is based on an effective crack length: $a + d_0$ including the fracture process zone length d_0, what is comparable with Irwin's plastic zone correction, with now a plastic and elastic hydrostatic stress field as fracture process zone, in stead of Irwin's plastic zone only. For $a = 0$, the clear wood strength is reached. This shows that the curve represents an extended, ultimate stress intensity criterion. A data fit to eq.(3.3) delivers the accountable dimensions of the fracture process zone. The slope of the curve eq.(3.3) is:

$$\frac{\partial \ln \sigma}{\partial \ln (a/d_0)} = \frac{\partial \ln (\sigma/\sigma_0)}{(d_0/a)\partial (a/d_0)} = \frac{a}{d_0} \frac{\partial \left(\ln (1 + a/d_0)^{-0.5} \right)}{\partial (a/d_0)} = \frac{-0.5}{1 + d_0/a} \tag{3.5}$$

This slope is: -0.5 for $a \gg d_o$ and this slope is zero when $a = 0$. Eq.(3.3) shows that for the whole curve LEFM applies and it is an indication that, at zero open crack dimensions, thus for: $a = 0$, the clear wood ultimate stress theory still follows LEFM, because it applies also for the constant initial length d_o (i.e. a constant fracture process zone length).

Weibull crack tip curvature size effect of wide angle notched beams

The derivation of the size effect on fracture strength clearly shows the necessity to regard the determining influence of both, the crack length a as well as the crack width (b or, related, crack tip curvature ρ) in any fracture mechanics analysis. Textbook equations should be adapted to account for both as done in this article for all discussed items. The application of geometrically similar specimens did show that there is no volume effect of the strength, when sharp cracks are determining for failure, because the mutual same volume of the fracture process zone is determining for fracture in all cases. This does not apply for wide angle notches (above 90^0 angle), because then there is not a strong concentrated process zone. The derivation of a volume effect due to a wider strength determining fracture

12

zone and even a total beam volume effect is given in [2] at the derivation of the strength of these wide angle notched beams. In [2], chapter 9, the essence of the derivation is discussed. The strength of the notched wooden beam is described by the probability of having a critical initial small crack density. This effect is opposed by toughening by the probability of having a less critical wide-angle crack tip curvature. This toughening effect, is therefore different at the different wide angles, showing different relative high stressed areas of the beam and thus different influences of the volume effect. This is shown to explain the other power of the depth than 0.5 for the strength, depending on the wide-notch angle.
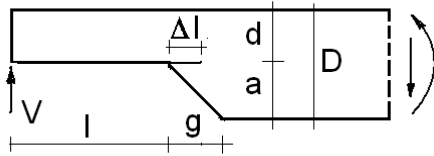

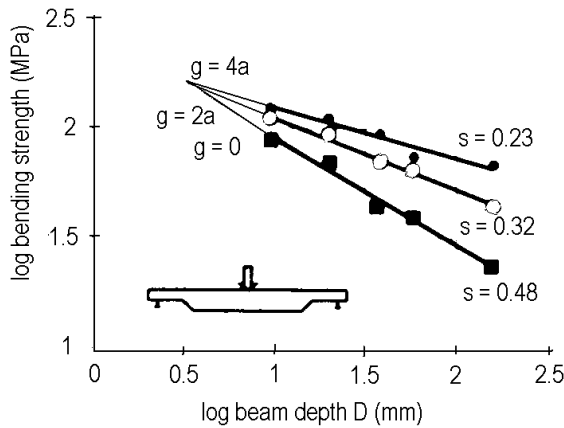*Fig. 2. Wide angle notched beam element [10a].*

Fig. 3. Measured bending strengths for different notch angles [*10a*]

The analysis of the strength of notched beams can be based on the energy method (called compliance method), [2], where the critical fracture energy is found from the difference of the work done by the constant force due to its displacement by a small crack extension minus the increase of the strain energy due to that displacement. According to this approach of [2], the bending stress σ_m at the end of the notched beam at $l = \beta D$ in Fig. 2 is:

$$\sigma_m = \frac{6V_f \beta D}{b(\alpha D)^2} \approx \frac{\sqrt{6EG_c / D}}{\sqrt{(\alpha - \alpha^4)}} ,$$
(4.1)

where $d = \alpha D$ when the notch is not close to the support. In [10a] is chosen in fig.2: $\alpha = d/D = 0.5$, what means that $d = a$. Further the length is $l = 2D$ when $g/a = 0$ and 2, while $l =$

13

$4D$ for $g/a = 4$ in Fig. 2, E is the modulus of elasticity and G_c the critical energy release rate. Eq.(4.1) applies for the rectangular notch ($g = 0$). For wide notch angles a more complicated expression applies because of the changing stiffness over length Δl of the crack extension. However, for given dimensions and loading, the basic form of the equation is the same as eq.(4.1), thus:

$$\sigma_m = B\sqrt{EG_c / D} \qquad (4.2)$$

where B is a constant depending on dimensions and notch angle. According to [1] and [2] is, as mentioned, $\sqrt{(EG_c)} \leftrightarrow Kc \leftrightarrow \sigma_t\sqrt{(r)}$ where σ_t is the equivalent cohesion strength and the crack tip radius r is the only parameter of the notch strength. The volume effect, depending on the stress, follows from § 9.3 of [2] and the analysis thus can be based on the yield stress and the characteristic volume around the notch tip, For the probability of a critical value of r, of the small initial cracks within the high stressed characteristic volume around the notch tip, the probabilistic reasoning of § 9.3 of [2] can be repeated as follows. The probability of having a critical flaw curvature $1/r$ in an elementary volume V_0 is equal to $1- P_0 (1/r)$, when P_0 is the survival probability. For a volume V containing $N=V/V_0$ elementary volumes the survival probability is in the same way:

$$P_s(V) = \exp\left(-NP_0\right) = \exp\left(-\frac{V}{V_0}\left(\frac{r}{r_0}\right)^{-k}\right) \qquad (4.3)$$

where, $P_0 (1/r) = (r_0/r)^k$ because the power law may represent any function in $1/r$. At "flow", this probability is not a function of σ, but of the flow strain, given by a critical r. Equal exponents for the same probability of failure in two cases now lead to:

$$r = r_s\left(V / V_s\right)^{1/k} \qquad (4.4)$$

and eq.(4.2) becomes:

$$\sigma_m \approx \frac{B'\sigma_t\sqrt{r_s}}{\sqrt{D}} \cdot \left(\frac{V}{V_s}\right)^{1/2k} \quad \text{or:} \quad \sigma_m = \sigma_{m0}\left(\frac{D}{D_0}\right)^{-0.5}\left(\frac{V}{V_0}\right)^{1/2k} \qquad (4.5)$$

For the notch angle of 90°, ($g = 0$ in Fig. 2), or for smaller angles, the high stressed elastic region around the crack tip is, as the fracture process zone itself, independent of the beam dimensions. Thus in characteristic dimensions $V = b'l'h' = V_0$ and eq.(4.5) becomes:

$$\sigma_m = \sigma_{m0}\left(\frac{D}{D_0}\right)^{-0.5} . \qquad (4.6)$$

independent of a volume effect. For the widest notch angle of 166° ($g/a = 4$), there is a small

14

stress gradient over a large area and V is proportional to the beam dimensions. Thus:

V (:) $b \cdot d \cdot l = \gamma D \cdot \delta D \cdot \beta D = \gamma \cdot \beta \cdot \delta D^3$ and: $V/V_0 = (\gamma \delta \beta D^3 / \gamma \delta \beta (D_0)^3) = (D/D_0)^3$.

Thus is, with $1/k = 0.18$:

$$\sigma_m = \sigma_{m0} \left(\frac{D}{D_0} \right)^{-0.5+3/(2k)} = \sigma_{m0} \left(\frac{D}{D_0} \right)^{-0.23} \tag{4.7}$$

For the angle of 153.40°, ($g/a = 2$), the high stressed region dimensions becomes intermediate, thus proportional to the total dimensions b and D and:

$V/V_0 = (bdl)/(b_0 d_0 l) = \gamma \delta D^2 / \gamma \delta (D_0)^2 = (D^2/(D_0)^2$ and with $1/k = 0.18$ is:

$$\sigma_m = \sigma_{m0} \left(\frac{D}{D_0} \right)^{-0.5+2/(2k)} = \sigma_{m0} \left(\frac{D}{D_0} \right)^{-0.32} \tag{4.8}$$

It follows from Fig. 3, that the values of exponents of $-0.5, -0.32$, and -0.23 are the same as measured. The coefficient of variation of the tests must have been: $1.2 \cdot 0.18 = 0.22$, as common for wood. According to the incomplete boundary value solution of [10a], for each angle type alone, these values of the exponents were respectively $-0.437, -0.363$ and -0.327, thus, too far away from the measurements.

The explanation of no volume effect of sharp notches due to the invariant characteristic volume, independent of the beam dimensions, explains also why for very small beams, also for sharp notches, there is a volume effect because then all beam dimensions are restrictive for the characteristic volume. As known, the exponent may also change from -0.5 to -0.23 with decrease of common beam dimensions. The constant dimensions of the fracture process zone act as a relative increase of the plastic zone for decreasing test beam dimensions and it appears that toughening, by a less critical wide-angle crack tip curvature at wider angles explains this volume effect.

The lines in Fig. 3 intersect at the elementary Weibull volume wherefore the depth dimension is $10^{0.6} = 4$ mm with a material bending strength of 147 MPa.

LINEAR ELASTIC ESTIMATION OF DISSIPATED FRACTURE ENERGY

The applied stress on a material is always proportional to the linear elastic strain only. Empirical and mathematical estimation of dissipated energy, thus always is based on knowledge of the linear elastic property of the strain energy. By non-linear fracture mechanics, this is blocked, by prescribed, non linear elastic behavior, which is non-existent for structural materials. Non linear elastic behavior should be described as a reversible

structural change process, according to molecular deformation kinetics [5]. This means that this energy release, like for a damage process, has to be accounted to the fracture energy and that then linear elastic strain behavior is maintained in the analysis of the process.

When fracture occurs in a cantilever beam, which already is loaded by load P, and shows, due to this crack extension a deformation δ, at the loading point, see fig. 4, then the applied external work on the beam is P·δ and the increase of the elastic strain energy can linear elastic be calculated to be P·δ/2 because strain energy is not involved in fracture or damage or plastic dissipation. It thus follows that also the dissipated energy, as fracture energy is known as:

$$P·\delta - P·\delta/2 = P·\delta/2 \tag{4.1}$$

Fig. 4. Crack extension in a loaded cantilever beam.

which is equal to the linear elastic strain increase. Thus applied external energy minus the applied, thus increase of strain energy, is the fracture energy (at these conditions).

By non-linear fracture mechanics is wrongly stated that the whole area under the loading curve of a strength test recording, (which represents the applied external energy), gives the fracture energy. The equation above shows that half this value applies.

The same applies in general. When the external stresses are held constant during crack extension, the work done by these stresses is equal to twice the increase of the strain energy of the body. Thus the amount of once this increase of strain energy is available as fracture energy. When fracture breaks bonds over the whole crack length, the cut bonds release to zero, causing the crack to open. The released linear elastic strain energy thus can be calculated by the release of the loading of these bonds, from maximal to zero, or by calculating the crack closing energy from zero to maximum (as e.g. applied in finite element crack closure technique). This linear elastic crack closure thus delivers a linear elastic Stress Intensity K_C calculation of non linear plastic and fracture energy of the ultimate state. Important is the conclusion that fracture, at any load combination, always is caused by uniaxial tensile rupture of pure hydrostatic loaded bonds, as follows from the derivation of the mixed mode fracture criterion and that this results in the so called failure modes in shear and tension which are not failure, but crack opening deformation modes due to linear elastic strain energy release only. Thus a reversed linear elastic crack closure calculation delivers

the right restauration of the accountable linear elastic determined critical stress intensities K_{Ic} and K_{IIc}, and related fracture energy. Wrongly the crack opening deformation modes are regarded as fracture modes and it is wrongly assumed that these modes occur independent of each other and can be added up. This of course is against the exact solution of compatibility of displacements and against satisfying the mixed mode fracture criterion.

Fracture energy as half the area under the loading curve

When a test specimen is mechanical conditioned, a linear initial loading line is possible in a constant loading rate, or constant strain rate test. As long this line is straight, as line OA in Fig. 5, there is no damage. Crack extension starts here at point A. The fracture energy is found as follows: the area OAB, written as A_{OAB} represents the applied strain energy on the specimen at point A. During the quasi static crack extension from B to D in Fig. 5, the external load does work on the specimen of: A_{ABDC}. The strain energy after the crack extension at point C is A_{OCD} and the strain energy increase is:
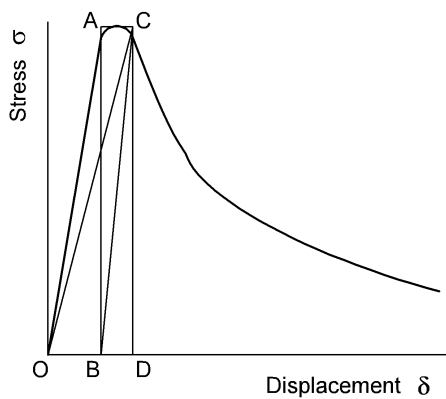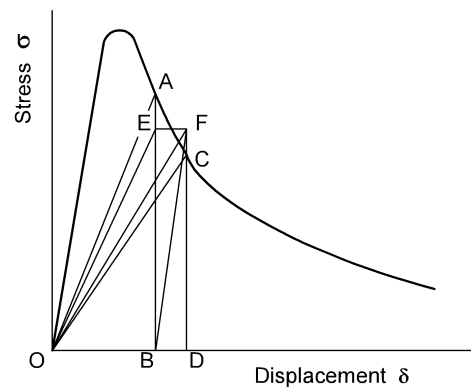

Fig. 5. Tension stress – displacement curve
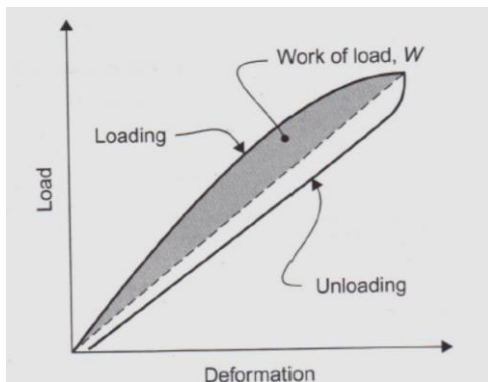

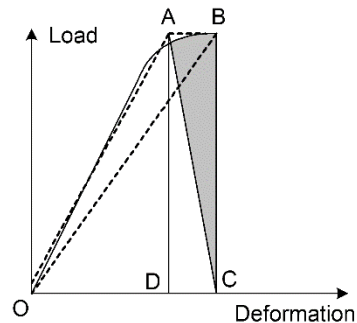Fig. 6. Descending stress –

Fig. 7. Mode II fracture energy

Fig 8

similarly mode I: Area: OABO = CABC = ABCD/2

17

$A_{OCD} - A_{OAB} = A_{OCD} - A_{OCB} = A_{CBD} = A_{ABDC}/2$

Thus half of the applied external energy is the amount of the applied strain energy and the other half thus is the fracture energy which is equal to this increase of strain energy. The same follows at unloading by yield drop. The fracture with unloading step AC in Fig. 6 (3.4.2) is energetic equivalent to the unloading steps AE and FC and the fracturing step EF at constant stress EB = FD = (AB + DC)/2. Thus. $A_{ABDC} = A_{EBDF}$

Identical to the case of Fig. 5, the increase in strain energy by crack extension in Fig. 6 (3.4.2) is: $A_{ODF} - A_{OBE} = A_{ODF} - A_{OBF} = A_{BFD} = A_{EBDF}/2 = A_{ABDC}/2$

equal to half the work done by the external load during crack propagation and thus also equal to the other half, the work of crack extension. It thus is shown that half the area under the curved load-displacement line represents the fracture energy.

Because, according to non-linear fracture mechanics, the whole area has to be accounted are K_I values of wood a factor 2 too high. For mode II, unstable fracture is expected after reaching the top so that there is no reliable stable unloading range and only A_{OACO} in Fig. 5 (3.4.1) can be accounted for wood what remains after subtraction of increase of strain energy A_{OCD}. Because, $A_{OAC} = A_{BAC} = A_{ABDC}/2$, thus is equal to half the area under the non-linear part of the load displacement curve, the right value is regarded and mode II data of wood need no correction. However, it is not sure that the top of the loading curve already was reached so that it is possible to have measured a too low value for K_{IIc}. Similar to Fig. 7 is the line OABO in Fig. 8 a hysteresis loop and A_{OABO} thus also is the fracture energy over the path AC. This is applied by the finite element method to measure fracture energy. Again a linear elastic estimation of non-linear behavior.

As mentioned there is no fracture or damage at a linear loading line (through the origin) at a constant loading rate or constant strain rate test. The strain energy at A, in Fig. 9, is A_{OAC}
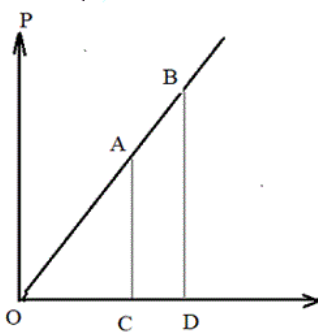

Fig. 9. Straight loading line

18

and the strain energy D is A_{OBD}. The difference in strain energy is A_{ABDC}. This is equal to the total applied external energy at the path C-D. There thus is no fracture.

CONCLUSIONS

A completion is given of the conclusions of the main article [1]. By discussion parameters, it is shown, that crack length a as well as the crack width b are determining and should be included in ultimate fracture equations.

● As shown, fracture always occurs by hydrostatic bonds failure at the crack tip and the crack is self similar, also for mixed mode failure.

● The given textbook stress equations thus only apply for $\theta = 0$ and for $r \rightarrow 0$. Therefore, stress intensities should be given in stead of the undetermined high hydrostatic stresses.

● It is shown that in linear and non-linear fracture mechanics linear elastic strain behavior is always essential and can not be missed.

● The Textbook boundary value analysis is restricted to pure shear loading along the crack and pure tension perpendicular to the crack. The combined, mixed mode, loading of tension plus shear is lacking and therefore there is no exact mixed mode failure criterion in Textbooks. This is corrected in [1] by the derivation eq.(4.1) to (4.13) and eq.(5.1) to (5.10) and the empirical verification. .

● Linear elastic behavior, Limit analysis up to the ultimate state of virtual flow, is shown to be the necessary approach of fracture mechanics as empirically confirmed by the linear elastic unloading and reloading behavior up to the ultimate stage.

● A lower bound solution then is based on equilibrium equations, stress boundary conditions which nowhere violate the yield condition. When there is an empirical confirmation and when this solution shows no discontinuity of displacements, the solution also is the exact solution.

Extended critical stress intensity criterion for sharp short cracks

● There is no need to regard, in the double logarithmic data plot of Fig. 1, that the horizontal line represents ultimate stress strength theory, the curved line represents fracture according to non-linear fracture mechanics, and the inclined straight line to represent linear elastic fracture mechanics. The whole curve follows the extended critical stress intensity criterion eq.(3.4) as extension of the long crack length eq.(3.1). Thus for short open cracks a, is the effective crack length $a + d_0$, including the process zone length d_0, and the distance of the

focus to the crack-tip r_o is extended to $r_o = 2\,d_0$, the new effective crack tip. This replaces Irwin's plastic zone correction by an elastic hydrostatic process zone correction.

Conclusions regarding size effects

● As example of the influence of the crack width parameter, the strength of wide angled notched beams is explained by the application of the Weibull type size effect in fracture mechanics. This is based on a critical small crack extension, opposed by a toughening effect, by a less high stressed wide crack tip zone, acting as a more extended lower stressed fracture process zone at wider crack tip angles.

● For sharp notch angles, up to 90°, there is no volume effect for full scale specimens, due to the constant characteristic volume, of the fracture process zone. Crack extension occurs at the notch tip. For wider notch angles, the peak stresses and stress gradients become lower and are divided over a larger region and influenced by the dimensions of the specimen and thus a volume effect correction applies.

● For very small beams, also for sharp notches, there is a volume effect because then the beam dimensions are restrictive for the characteristic volume.

● The intersect of the three lines in Fig. 3, with different values of "s" according to eq.(4.6) to (4.8), due to different boundary conditions, which can not apply at the same time for the different notch angles, thus can not be explained by a boundary value analysis. This intersect only can be explained to be due to the volume effect of the strength indicating failure by small crack extension within the high stressed region at the notch tip.

● It further explains why for very small dimensions of the test specimens, also for sharp notches, the volume effect applies.

● The lines in Fig. 3 intersect at the elementary Weibull volume wherefore the depth dimension is $10^{0.6} = 4$ mm with a material bending strength of 147 MPa.

Conclusion regarding linear elastic strain energy

● The proof is given that the fracture energy is equal to half the area under the curved part of a plot of a constant loading rate- or constant strain rate- test. This is based on the, by the plot directly calculable, linear elastic strain energy increase. Wrongly the whole area of the plot is claimed to be the fracture energy by non-linear fracture mechanics. For wood therefore, the mode I stress intensities in Textbooks are a factor 2 too high. As shown, the same does not apply for mode II, where the right plot area is accounted.

REFERENCES

[1] van der Put TACM. Necessary Corrections of the Mathematical Foundation of Fracture Mechanics, *Int J Fract Damage Mech.* 2020 16 – 45.

[2] van der Put TACM. *A new fracture mechanics theory of wood, second extended edition*, Nova Science Publishers, Inc. New York, 2011.

[3] Anderson TL. Fracture Mechanics, Fundamentals and applications CRC Press Taylor & Francis Group, third edition 2005.

[4] Jaeger JC, Cook NGW, Zimmerman RW. Fundamentals of Rock Mechanics. Blackwell Publishing, 4th ed. 2007.

[5] van der Put TACM. Deformation and Damage Processes in Wood. Doct. thesis, Delft University Press 1989.

[6] Inglis CE. Stresses in a plate due to the presence of cracks and sharp corners. Read at In Nava Arch, 54th session 1913.

[7] Wu EM. Application of fracture mechanics to anisotropic plates ASME J Mech Series E 34,4 1967 pp 967 - 974 .

[8] Smith I, Landis E, Meng Gong. *Fracture and Fatigue in Wood, § 4.3*, John Wiley, Chichester, West Sussex PO 19 8SQ

[9] Bazant ZP. (1999) Size effect on structural strength: a review. Archive of Applied Mechanics; 69: 703-725.

[10] Leicester RH. *Design specifications for notched beams in AS 1720*, CIB-W18/38-6-1, meeting 38, Karlsruhe, Germany, August 2005.